ARTICLE

Peptide-Mediated Reduction of Silver Ions on Engineered Biological Scaffolds

Ki Tae Nam,[†,⊥] Yun Jung Lee,[†,⊥] Eric M. Krauland,[‡] Stephen T. Kottmann,[§] and Angela M. Belcher[†,‡,*]

[†]Department of Materials Science & Engineering, [‡]Department of Biological Engineering, and [§]Department of Chemistry, Massachusetts Institute of Technology, Cambridge, Massachusetts 02139. [⊥]These authors contributed equally to this work.

ABSTRACT Herein we report the spontaneous reduction of silver ions into nanostructures by yeast surface-displayed glutamic acid (E_6) and aspartic acid (D_6) peptides. Light spectroscopy and electron microscopy reveal that silver ions are photoreduced in the presence of the polycarboxylic acid-containing peptides and ambient light, with an increase in reduction capability of E_6 expressing yeast over D_6 yeast. The importance of tethering peptides to a biological scaffold was inferred by observing the reduced particle forming capacity of soluble peptides with respect to corresponding yeast-displayed peptides. This principle was further extended to the M13 virus for fabrication of crystalline silver nanowires. These insights into the spontaneous reduction of metal ions on biological scaffolds should help further the formation of novel nanomaterials in biological systems.

KEYWORDS: nanomaterials · yeast · biomineralization · M13 bacteriophage · silver · reduction · peptide conformation

Biological systems have developed biomineralization processes to nucleate, grow, and assemble inorganic materials.[1,2] Examples of biomineralized products include pearls, bone, keratin, shell, calcite, siliceous materials synthesized by diatoms[3] and sponges,[4] and magnetite in magnetotatic bacteria.[5] An important component of biomineralization is the protein or peptide template that controls the shape and crystal structure of biominerals as well as the assembly behavior. The extraction of nucleating biomolecules from the biominerals and the identification of materials specific peptides through combinatorial approaches[6–8] have broadened the possible application of biomineralization in nanoelectronics and nanobiotechnology. The underlying mechanism can be applied to the synthesis of technologically important materials beyond those few existing biominerals in nature. Peptides have been engineered to grow and assemble[9] semiconductor, magnetic,[10] metal oxide nanomaterials,[11] and we extend this approach to the spontaneous reduction of silver by introducing peptide sequences on yeast and M13 viruses to facilitate the growth of templated silver nanostructures.

Organisms such as bacteria[12] and fungi[13] are reported to synthesize silver particles intra- or extracelluarly when they are exposed to silver salts. Although there is growing interest in the bioinspired synthesis of silver nanoparticles, a general understanding of growth is not yet known. Recently, the role of specific peptide motifs has been explored through identification of dodecamer peptides that are reported to generate silver nanoparticles of various morphology.[14] The importance of peptides was demonstrated as studies with single amino acid solutions of lysine, proline, serine, and arginine showed them to be incapable of silver reduction.[14] Additionally, tryptophan and aspartate, which can be used as reducing agents in the synthesis of gold nanoparticles, did not show the ability to reduce silver ions.[15] Although it has been experimentally demonstrated that the biological system such as cells, enzymes, and peptides can reduce the metal ions, the detailed mechanisms are not well understood. The conformation, overall charge, and functional groups of biomolecules may all contribute to biological reduction in conjunction with solution pH, light, temperature, and other ions in solution.

As an effort to contribute to the understanding of spontaneous reduction, we focus on the role of carboxylic acid containing peptides expressed on yeast surfaces. Yeast surface display provides a convenient model system for the study of genetically engineered biomolecules with inorganic materials[16] while carboxylic acid groups are known to coordinate metal ions which may act as a nucleation site for nanoparticle formation.[17–19] Additionally, glutamic and

*Address correspondence to belcher@mit.edu.

Received for review January 10, 2008 and accepted June 16, 2008.

Published online July 1, 2008.
10.1021/nn800018n CCC: $40.75

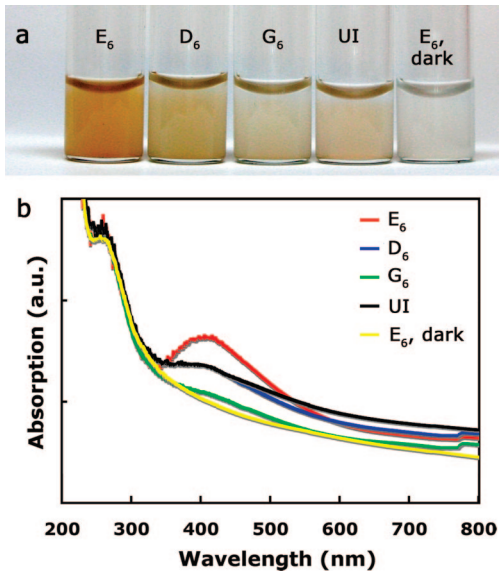

Figure 1. Characterization of yeast solutions incubated in 1 mM $AgCOOCH_3$ solution. Yeast cell concentration is 1 O.D. Yeast solutions are named for corresponding clones. Expressed peptides are E_6, hexaglutamic acids; D_6, hexaaspartic acids; G_6, hexaglycine acids; UI, uninduced clone with no surface expressed peptides; E6 dark, hexaglutamic acids incubated in the dark. (a) Photograph of the yeast solutions shows the color change resulting from silver nanoparticles formation. (b) UV−vis absorption spectra of the same solutions. Peak at 260 nm comes from DNA of yeast cells

aspartic-acid-rich peptides play an important role in biomineral growth as evident in the high population in biomineralizing protein sequences. While previous research has studied long polypeptide chains or single amino acids, this work utilizes hexamer peptides that are short enough to deduce side-chain influence while long enough to have multivalent interactions. Additionally, previous reports of silver biomineralization occur in the solution with minimal control over the spatial distribution. In this work, the genetically engineered yeasts not only mediate the reduction of silver ions through expressed peptides, but also act as templates for controlled spatial growth of particles. Specifically, our findings demonstrate spontaneous reduction of silver facilitated by carboxylic acid groups in the presence of ambient light. The principle of the peptide-mediated reduction elucidated by the engineered yeast was further extended to a filamentous M13 virus scaffold for fabricating crystalline silver nanowires.

RESULTS AND DISCUSSION

When the hexaglutamic acid expressed (clone named as E_6) or hexaaspartic acid expressed (clone named as D_6) engineered yeasts were incubated in an aqueous solution of $AgOOCCH_3$ for 24 h at room temperature, the solution turned an orange color as shown in Figure 1a. Reduction of the silver ions was evident by a gradual and steady increase of the reddish color. The characteristic reddish color of the solution and absorption peak at ~400 nm are due to surface plasmon resonance of silver nanoparticles and are dependent on the size and shape of the particles. Interestingly, without any known reducing agent in solution, silver ions were bioreduced by the genetically engineered yeast. Contrary to E_6 or D_6 yeasts, little color change was seen for yeast expressing hexaglycine (clone named as G_6) (Figure 1b), and solutions without yeast did not show any color change. To prevent the buffer mediated reduction, all our experiments were conducted in purified water (Millpore Mill-Q, 18.2 MΩ-cm) without the presence of any buffer salts. These control experiments indicate that the carboxylic acid groups of glutamic acid or aspartic acid are involved in the reduction of silver ions. Typically, the carboxylic acid groups in block copolymer systems have been utilized for silver deposition because of their binding affinity to positive silver ions. However, in all the cases, the post-treatment with a reducing agent, such as H_2[19] and $NaBH_4$,[20] or UV[18] and γ- radiation,[21] was necessary. To our knowledge, there is no prior report of carboxylic-acid-mediated silver reduction in water at ambient conditions. A previous report about silver nanoparticles organization on tobacco mosaic virus (TMV)[22] showed the importance of glutamate and aspartate in site-specific mineralization of silver, but contribution of these peptides to the silver reduction itself was not considered. To understand the reduction mechanism, we conducted control experiments in which the mixtures were kept in the dark. Interestingly, even after a few days, no reduction was evident in these samples (Figure 1). All the control reactions were also conducted with rocking to prevent cell sedimentation. Conversely, mixtures kept under ambient light but with UV energy-blocking polymer coatings exhibited significant silver reduction. This polymer coating effectively blocked UV light with wavelengths below 300 nm. To further reduce the effect of UV light, the same experiments were done under white fluorescent light in a dark room. The solution also showed significant silver reduction. (Supporting Information, Figure S1). This result suggests that the reduction of silver ions is the cooperative result of the carboxylic acid and ambient light. Among ambient light, it would be visible light that assumes the most significant role in the reduction process. Even though the uninduced cells, named UI, expressed no surface peptides, the yeast solution changed colors with an absorption peak comparable to D_6. However, the adsorption peak in E6 samples is much higher than that in the uninduced sample. In the case of sample UI, the reduction of silver ion is possibly due to a negative charge and the presence of polysaccharide on the yeast surface. Previously other groups demonstrated that polysaccharides and their derivatives are shown to photochemically synthesize metal nanoparticles such as gold and silver[23−25] using UV light as a reducing agent. However, the growth of silver particles with uninduced cells was less controlled than that with peptide-assisted nucleation, as witnessed by further electron microscopy analysis. Furthermore, the electron microscopy analysis using TEM and SEM is believed to be more

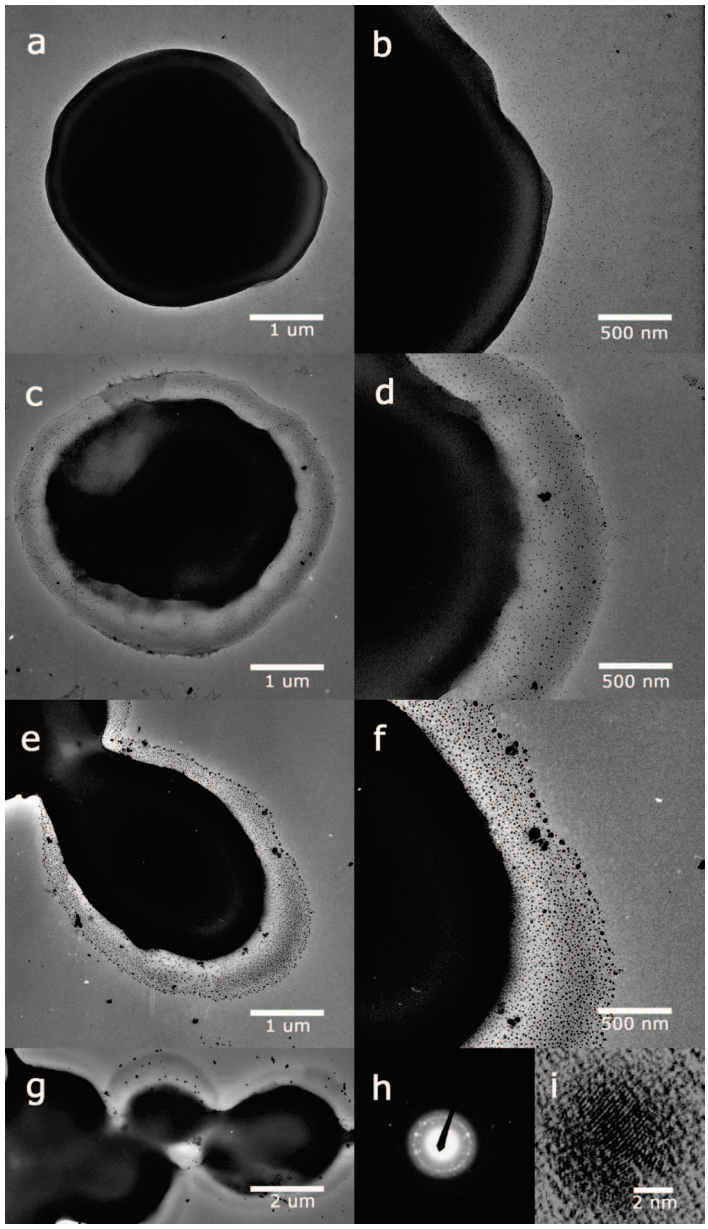

Figure 2. TEM analysis of silver reduction by engineered yeast. For all solutions, yeast cell concentration is 1 O.D. and $AgOOCCH_3$ concentration is 1 mM: (a) uninduced (UI); (b) UI high magnification; (c) D_6; (d) D_6 high magnification; (e) E_6; (f) E_6 high magnification; (g) low magnification image of E_6 showing several cells coated with silver nanoparticles layer; (h) electron diffraction pattern confirms the crystalline nature of the silver nanoparticles; (i) high resolution TEM image of silver nanoparticles.

accurate than the UV−vis absorbance in comparing the reduction capability.

Transmission electron microscopy (TEM) analysis (Figure 2c−g) showed homogeneous silver nanoparticles with sizes of approximately 10−20 nm coated on the cell wall of yeast expressing peptides. Consistent with the color change and UV−vis absorption spectroscopy trends, the average particle size was larger and the distribution density greater for the E_6 than for the D_6 solution. An electron diffraction pattern (Figure 2h) and a high resolution TEM (HRTEM) image (Figure 2i) confirmed that the particles coating the yeast were crystalline silver nanoparticles. The silver nanoparticles were not aggregated but stabilized by the expressed peptides. For the uninduced yeast (Figure 2a,b), the morphological features were quite different from that of induced ones. No obvious coating layer was observed and silver nanoparticles were not bound to the surface of the yeast and aggregated to large irregular particles (Figure S2).

As mentioned above, the silver ion reduction in this case could have been mediated by the negative charge or polysaccharide of the yeast surface. It is likely that the silver nanoparticles formed by polysaccharides were not strongly bound to the yeast surface because of the weak interaction between the silver particles and the polysaccharides.[23] This could also explain why the number of silver nanoparticles near the yeast surface was much less than that of D_6 even though UV−vis absorption and color change were similar. Scanning electron microscopy (SEM) analysis (Figure 3a−c, e−g) also demonstrates that engineered yeast provided a template for silver nanoparticle growth and the density of nanoparticles could be controlled by means of genetic engineering of expressed peptides. Silver nanoparticles appeared as bright dots due to their electron dense metallic character. Conversely, a lack of nanoparticles was noticed in E_6 yeast not exposed to silver solution (Figure 3d and 3h).

These results suggest that the combination of carboxylic acid-containing peptides and ambient light facilitate the reduction of silver into nanoparticulates. Although an exact photoreduction mechanism is still under investigation, we believe that the energy barrier for silver reduction is lowered when silver atoms are bound to peptides containing carboxylic groups. Carboxylic groups are nucleophilic such that their binding with silver ions induces partial electron transfer displacing the Fermi level of silver cluster toward the more negative potentials. This hypothesis is supported by experimental results from other groups. It was reported that when silver ions are bound to carboxylic acid group, UV photoreduction of silver ion become more facile.[26] In this regard, silver ion binding to carboxyl groups catalyzes the reduction of silver ions, as in the case of silver ion-catalyzed amine oxidation[27] and silver ion-catalyzed amino acid oxidation.[28] We believe that water could be an electron source for the initial nucleation of silvers. Recently, solvated electrons in water have been observed[29] as well as water dissociation mechanisms, which may account for these water-derived electrons. Like the proposed mechanism in photochemical reductions of Fe(III) complexes of polycarboxylates, the carboxylate radical activated by the visible light can be possibly involved.[30] In our system, once a silver atom is formed, it becomes easier for silver ions to be photochemically reduced due to the increased reduction potential of silver clusters and metallic characteristic of silver atoms. However, the exact mechanism is still under investigation.

Surprisingly, silver ions exposed to E_6 yeast result in greater nanoparticle formation than those exposed to D_6 yeast. Assuming a similar binding affinity of Ag^+ to the carboxylic acid, the different reduction kinetics appears counterintuitive. To understand differential reduction between E_6 and D_6 yeast, we explored the local conformation of these peptides. When present as an individual neutral amino acid, silver ion affinity of glutamate was calculated to be slightly higher than aspartic acid using hybrid density functional theory.[31] This difference may be amplified when aggregated over six residues. In addition, Monte Carlo simulations show a structural difference between the peptides. The additional alkyl link in glutamic acid allows for slight increases in conformational freedom and nonpolar surface area, resulting in a more folded backbone conformation. This gives rise to a pocket-like structure in hexaglutamic acid (Figure S3), while hexaaspartic acid on average assumes a more linear conformation. We hypothesize that the pocket-like structure of E_6 peptides creates a greater local concentration of carboxylic acid residues and therefore, a greater level of silver ions. This may increase particle formation as the silver redox potential depends on the number of Ag in the cluster. The redox potential of a single silver ion is -1.8 V and increases as the atom number in a cluster increases up to 0.799 V for bulk silver.[32] Taken together, silver ions bound to carboxyl groups reduce more easily while simultaneously increasing the local concentration of silver ions, which may further reduce the energy barriers to reduction. As a result of these cooperative mechanisms, silver ions can be photoreduced by the carboxylic acid group even under ambient light.

The importance of fixing peptides to a biological template was demonstrated by observing the nanoparticle growth of soluble peptides. We tested the reduction ability of various concentrations of soluble hexaglutamic acid peptide in silver solution (1 nM−1 mM peptide solution, 1−8 mM $AgOOCCH_3$ solution). According to the absorption data, reduction was only observed at 1 mM peptide and 8 mM $AgOOCCH_3$ solution (Figure S4). Considering the approximate number of hexaglutamate peptides on the yeast (5×10^4 peptides/cell) and the yeast concentration (1 O.D. $\sim 2 \times 10^7$ cells/mL), the total concentration of the peptides expressed on all the yeasts in solution is $\sim 10^{12}$ peptides/mL. Conversely, the soluble peptide experiments at 1 mM contained 6×10^{17} peptides/mL. Indeed, there are no prior reports on the silver ion reduction mediated by soluble glutamic or aspartic acid peptides. Therefore, the fixing of the peptides in a biological scaffold on the yeast surface may be an additional factor in the reduction mechanism. Enhanced reaction rate has been observed before in other constrained systems including "membrane catalysis" [33,34]and "micelle catalysis"[35] when one of two reactants remains fixed on a two-dimensional surface. This may be explained by the increased collision probability of reactants toward a fixed target.[36–38] The yeast biological templates inherently provide a two-dimensional tethering effect, so we can expect more efficient reactions on our biological scaffolds. To further investigate peptide-mediated reduction, we expanded this rationale to template silver nanowires on an M13 bacteriophage surface that has increased surface peptide density.

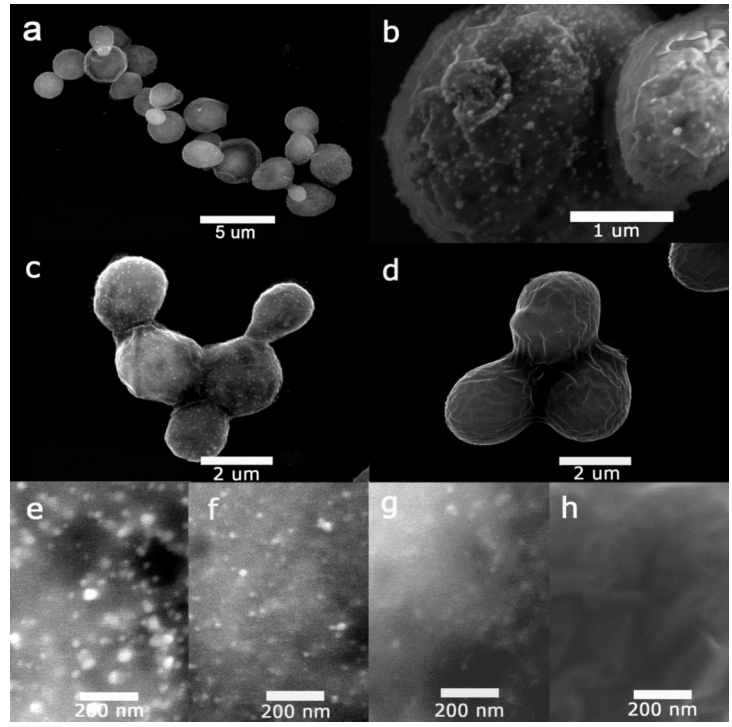

Figure 3. Scanning electron micrographs of yeast cells. The yeast solutions are prepared as those in Figure 2, except control sample. Control sample is pristine E_6 yeast not exposed to silver solution. (a−d) Low magnification images (5000−30000×) of yeast cells with carbon 10 nm coating layer: (a−c) E_6, (d) control sample. (e−h) High magnification images (80000×) without coating layer: (e) E_6, (f) D_6, (g) UI, (h) control sample. Yeast cells were not coated with conducting materials to visualize small particle features.

To template silver nanowires, we engineered a tetraglutamic acid peptide (-EEEE, called E4) onto the n-terminus of p8, the major coat protein of M13 bacteriophage. Roughly 2700 copies of the p8 major coat protein self-assemble into the capsid of the wild-type virus, resulting in 5 fold rotation symmetry along the length of virus. Previously, the E4 virus was utilized as a biological template to grow and assemble cobalt oxide nanowires for nanostructured Li ion battery electrodes.[11] There has also been an effort to coat TMV more densely with silver by genetic insertion of two cysteine residue, but the resultant template was not a fully covered nanowire but a string of nanoparticles.[39] In their study, the spacing between nearest neighbor peptides expressed for TMV is similar to that of M13 virus. We speculate that the different concentration of metal ions and viruses and the different binding character may explain the difference in morphology in those

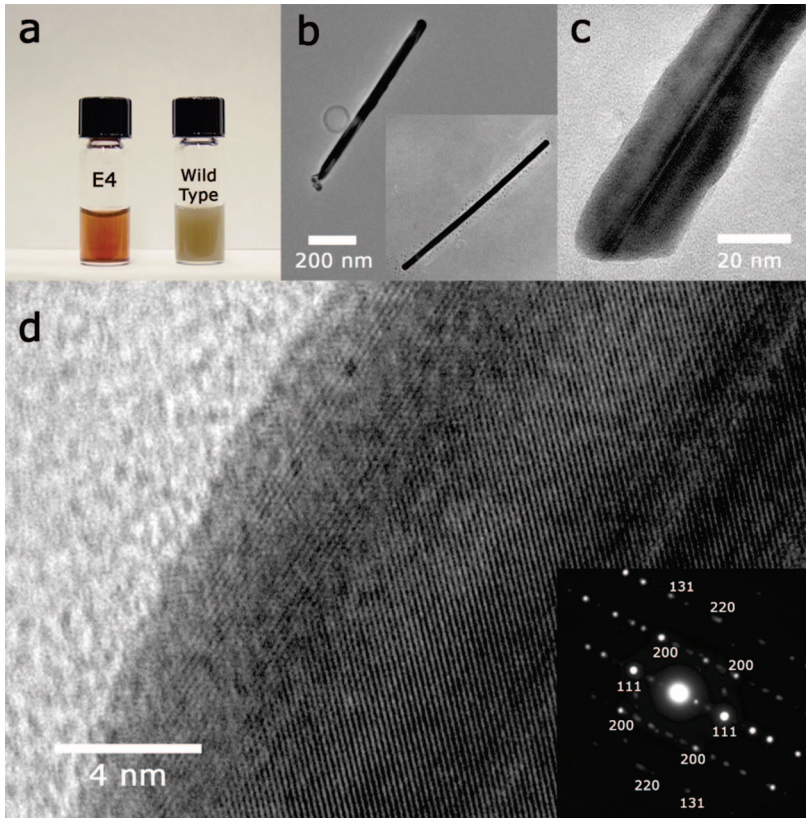

Figure 4. Silver reduction by engineered virus: (a) photographs of the silver solution reduced by E4 virus (left) and wild-type virus; (b) TEM image of the virus-based silver wires; (c) high resolution TEM image of the virus-based silver wire; (d) high resolution TEM image of the virus-based silver wire and diffraction pattern (inset).

two studies. We anticipate that the higher density of glutamate expressed on peptides of the engineered M13 bacteriophage (as compared to that of the yeast) can lead to the formation of nanowires. Indeed, computational simulation of p8 protein assembly shows that the distance between the helically arranged nearest neighbors of the tetraglutamate is around 3 nm at 100% incorporation.

When E4 virus was incubated in an aqueous solution of 1 mM silver acetate for two hours at room temperature, the solution turned red as shown in Figure 4a. The appearance of a red color clearly indicated the reduction of silver ions. Alternatively, a silver solution incubated with wild-type phage (M13KE) exhibited a turbid yellow color and revealed that large and irregular precipitates were formed. UV−vis spectra showed no absorption peak between 200 and 800 nm. The reduction of silver ions by wild-type viruses was presumably due to the negatively charged surface of the virus[40] as with the yeast surface.

TEM analysis shows the detailed structure of nucleated silver on the virus particles. Wire-like structures were observed along the length the E4 (Figure 4b). Conversely, wild-type virus produced large and irregular silver particles (Figure S5). The length of silver wires on the E4 virus corresponds to the length of the virus particles, and the thickness is approximately 30 nm. The high resolution TEM image in Figure 4d shows the silver wire formed on the E4 virus. The crystallographic structure of silver wires made by the E4 virus was determined by SAED in combination with HRTEM.

A diffraction image (Figure 4d) shows that the single crystal patterns of <100> and <112> are superimposed. Diffraction spots from (200), (020), and (220) planes of square symmetry correspond to the [001] zone while the (111), (220), and (311) diffraction spots of rectangular symmetry correspond to the [112][22] zone. The additional spots can be explained by double diffraction. This analysis suggests that five {111} twin boundaries are located cyclically with *D5h* symmetry along the longitudinal axis of Ag wire.[41] The formation of the crystals may be associated with the highly oriented p8 proteins and the 5-fold symmetry of the arrangement of p8 proteins. The nucleation and growth process seem to have an analogy to the molecular epitaxy in biomineralization[42] and epitaxial growth in vacuum technology. In contrast, we previously reported the regulation of the crystal orientation on the viruses where the textured assembly of nanoparticles was transformed into single crystal nanowires *via* heat-annealing based on the mechanism of orientated aggregation-based crystal growth.[10] Here, the higher density of incorporated peptides allows the nucleated silver to grow in the thermodynamically most favorable single crystalline form without postannealing on the scaffold.

CONCLUSIONS

The genetically engineered scaffolds not only mediate the reduction of silver ions but also act as templates for the synthesis of nanostructures. Our results demonstrate that short peptides containing carboxylic acid functional groups facilitate reduction under ambient light and the reduction ability is dependent on the local concentration of silver ions associated with the conformation of peptide. Additionally, this study suggests that tethering peptides to a biological scaffold enhances the reduction ability, and the surface density of the peptides on the scaffold determine the final nanostructure of silver. We anticipate that this study will contribute to the understanding of the spontaneous reduction of metal ions in biological systems and facilitate the implementation of environmentally benign biological methods for fabricating technologically important nanomaterials.

METHODS

Genetic Engineering of Yeast Displayed Peptides. Hexamer peptides were engineered onto the surface of yeast as previously described.[16] Briefly, peptides were displayed as fusions to the C-terminus of Aga2, which is encoded on a 2-μm plasmid downstream of a Gal-based promoter. The expression vectors were maintained in *S. cerevisiae* strain EBY100, which has Aga1 under control of a Gal-based promoter integrated in its genome, as previously described.[16] Peptide expression vectors (X_6) were generated from annealed oligonucleotides (*i.e.*, G_6 peptide oligos: 5′GTGGCggtggtggtggtggcggaTAGCCAGTAGC and 5′CTGGCTAtccgccaccaccaccaccGCCACCGCC) with BstXI compatible sticky ends ligated into BstXI sites of expression vector pBPZ. The complete list of oligonucleotides used is available upon request. All vectors were amplified, sequenced, and then transformed into EBY100. Peptide expression was induced by growing cells at mid-log phase in Select-Galactose media at 30 °C for 18−24 h.

Silver Reduction by Yeast. Among various silver salt precursors, silver acetate ($AgOOCCH_3$) salt was chosen because metal ions from acetate salt were found to load faster and to a greater extent within block copolymer containing carboxylic acid group than metal ions from chlorides, nitrates, and sulfates.[17] In addition, the silver ion reduction rate constant from silver formate (AgOOCH), which has almost the same structure as $AgOOCCH_3$, was reported as higher than that of Ag_2SO_4 and $AgNO_3$.[18] Silver acetate salt (99% pure) was obtained from Alfa Aesar. In a typical experiment, engineered 1 O.D. (O.D. is equivalent to absorbance units at 600 nm) yeast cells (10^6−10^7 cells) were washed 3 times in 1 mL of Millipore water and incubated in 1 mM aqueous solution of $AgOOCCH_3$ for 24−90 h at room temperature under ambient light. To prevent buffer-mediated reduction, all experiments were conducted in purified water.

The sample was agitated *via* rocking to avoid yeast cell sedimentation. For control experiments in which the mixtures were kept in the dark, the vials were wrapped with aluminum foil and placed in the dark room. These samples were analyzed by UV−vis absorption spectroscopy, TEM (JEOL 200CX TEM and JEOL 2010 TEM) and environmental SEM (FEI/Philips XL 30 FEG-ESEM). For TEM analysis, solutions were dropped on the copper grid, washed with distilled water several times, and dried. For SEM specimen preparation, yeast cells were first settled on a silicon substrate. After 4 hours fixation with 2% (v/v) glutaraldehyde, 2% (v/v) paraformaldehyde, 5% sucrose in 0.1 M sodium cacodylate buffer, the specimen was rinsed in distilled water, dehydrated in 100% dry ethanol, and critical-point dried in CO_2. Specimens were examined in FEI/Philips XL 30 FEG-ESEM with and without surface carbon coating layers.

Genetic Engineering of M13 Virus and Silver Reduction by the Engineered Virus. To display tetraglutamic acid (-EEEE) on the n-terminus of the p8 protein on M13 bacteriophage (producing so-called E4 phage), a small DNA duplex encoding the amino acids was made using an oligonucleotides 5′-CTACTACAAGGATCCTCCTCCTCCTCTGCAGCGAAAGACAGCA-3′ and the extension primer, 5′-GATGCTGTCTTTCGCTGCAG-3′. The duplex was digested with *Pst*I and *Bam*HI and ligated into M13SK phage vector, and confirmed by DNA sequencing. The E4 phage was incubated in an aqueous solution 1 mM $AgOOCCH_3$ for 2 hours at room temperature under ambient light. All experiments were performed in purified water and E4 phage was dialyzed against purified water overnight to prevent buffer effect. These samples were analyzed by UV−vis absorption spectroscopy and TEM (JEOL 200CX TEM and JEOL 2010 TEM). For TEM analysis, solutions were dropped on the copper grid, washed with distilled water several times and dried.

Molecular Simulation of the Hexamer Peptides (Figure S3). Monte Carlo (MC) simulations of the hexamer peptides were performed using the OPLS-AA force field (Jorgensen, W.L., MCPRO, Version 1.68, Yale University, New Haven, CT, 2002). The effects of the aqueous solution environment were included through a solvation energy term in the Monte Carlo energy calculation. The solvation energy of each peptide conformation was calculated as the sum of a polar term, evaluated from the solution of the Poisson−Boltzmann equation, and a nonpolar term modeled as proportionate to the molecular surface area.
Poisson−Boltzmann calculations were carried out using a multigrid solver with a grid spacing of 0.3 A. Atomic charge and radius parameters were taken from the OPLS-AA force field. Internal and external dielectric constants were set to 1 and 80, respectively, in order to remain consistent with the OPLS force field. Each simulation included equilibration for 100k MC steps prior to averaging over 1 M MC steps in the NPT ensemble. Conformations were saved periodically from the resulting ensemble and subsequently used to evaluate average properties of the peptides.

Acknowledgment. This work was supported by the Army Research Office Institute of Collaborative Biotechnologics (ICB).

Supporting Information Available: UV−vis absorption spectra of E6 yeast solution incubated with 1 mM $AgOOCCH_3$ under white fluorescent light with and without UV blocking polymer (Figure S1); TEM images of silver nanoparticles synthesized by uninduced yeast solution (Figure S2); graphical representation of average conformation of D6 and E6 hexamer from Monte Carlo Simulation (Figure S3); analysis of silver reduction by soluble hexaglutamic acid peptide by UV−vis absorption spectra at various peptide and $AgOOCCH_3$ concentration (Figure S4); and TEM images of silver nanoparticles produced by wild-type M13 viruses (Figure S5). This material is available free of charge via the Internet at http://pubs.acs.org.

REFERENCES AND NOTES

1. Mann, S. *Biomimetic Materials Chemistry*; VCH: New York, 1996.
2. Weiner, S.; Addadi, L.; Wagner, H. D. Materials Design in Biology. *Mater. Sci. Eng., C* **2000**, *11*, 1–8.
3. Poulsen, N.; Sumper, M.; Kroger, N. Biosilica Formation in Diatoms: Characterization of Native Silaffin-2 and Its Role in Silica Morphogenesis. *Proc. Nat. Acad. Sci. U.S.A.* **2003**, *100*, 12075–12080.
4. Cha, J. N.; Shimizu, K.; Zhou, Y.; Christiansen, S. C.; Chmelka, B. F.; Stucky, G. D.; Morse, D. E. Silicatein Filaments and Subunits from a Marine Sponge Direct the Polymerization of Silica and Silicones in Vitro. *Proc. Natl. Acad. Sci. U.S.A.* **1999**, *96*, 361–365.
5. Scheffel, A.; Gruska, M.; Faivre, D.; Linaroudis, A.; Plitzko, J. M.; Schuler, D. An Acidic Protein Aligns Magnetosomes along a Filamentous Structure in Magnetotactic Bacteria. *Nature* **2006**, *440*, 110–114.
6. Brown, S. Metal-Recognition by Repeating Polypeptides. *Nat. Biotechnol.* **1997**, *15*, 269–272.
7. Whaley, S. R.; English, D. S.; Hu, E. L.; Barbara, P. F.; Belcher, A. M. Selection of Peptides with Semiconductor Binding Specificity for Directed Nanocrystal Assembly. *Nature* **2000**, *405*, 665–668.
8. Sarikaya, M.; Tamerler, C.; Jen, A. K. Y.; Schulten, K.; Baneyx, F. B: Nanotechnology through Biology. *Nat. Mater.* **2003**, *2*, 577–585.
9. Yoo, P. J.; Nam, K. T.; Qi, J. F.; Lee, S. K.; Park, J.; Belcher, A. M.; Hammond, P. T. Spontaneous Assembly of Viruses on Multilayered Polymer Surfaces. *Nat. Mater.* **2006**, *5*, 234–240.
10. Mao, C. B.; Solis, D. J.; Reiss, B. D.; Kottmann, S. T.; Sweeney, R. Y.; Hayhurst, A.; Georgiou, G.; Iverson, B.; Belcher, A. M. Virus-Based Toolkit for the Directed Synthesis of Magnetic and Semiconducting Nanowires. *Science* **2004**, *303*, 213–217.
11. Nam, K. T.; Kim, D. W.; Yoo, P. J.; Chiang, C. Y.; Meethong, N.; Hammond, P. T.; Chiang, Y. M.; Belcher, A. M. Virus-Enabled Synthesis and Assembly of Nanowires for Lithium Ion Battery Electrodes. *Science* **2006**, *312*, 885–888.
12. Klaus, T.; Joerger, R.; Olsson, E.; Granqvist, C. G. Silver-Based Crystalline Nanoparticles, Microbially Fabricated. *Proc. Natl. Acad. Sci. U.S.A.* **1999**, *96*, 13611–13614.
13. Mukherjee, P.; Ahmad, A.; Mandal, D.; Senapati, S.; Sainkar, S. R.; Khan, M. I.; Parishcha, R.; Ajaykumar, P. V.; Alam, M.; Kumar, R.; *et al.* Fungus-Mediated Synthesis of Silver Nanoparticles and Their Immobilization in the Mycelial Matrix: A Novel Biological Approach to Nanoparticle Synthesis. *Nano Lett.* **2001**, *1*, 515–519.

14. Naik, R. R.; Stringer, S. J.; Agarwal, G.; Jones, S. E.; Stone, M. O. Biomimetic Synthesis and Patterning of Silver Nanoparticles. *Nat. Mater.* **2002**, *1*, 169–172.
15. Selvakannan, P. R.; Swami, A.; Srisathiyanarayanan, D.; Shirude, P. S.; Pasricha, R.; Mandale, A. B.; Sastry, M. Synthesis of Aqueous Au Core-Ag Shell Nanoparticles Using Tyrosine as a pH-Dependent Reducing Agent and Assembling Phase-Transferred Silver Nanoparticles at the Air-Water Interface. *Langmuir* **2004**, *20*, 7825–7836.
16. Peelle, B. R.; Krauland, E. M.; Wittrup, K. D.; Belcher, A. M. Design Criteria for Engineering Inorganic Material-Specific Peptides. *Langmuir* **2005**, *21*, 6929–6933.
17. Clay, R. T.; Cohen, R. E. Synthesis of Metal Nanoclusters within Microphase-Separated Diblock Copolymers: Sodium Carboxylate vs Carboxylic Acid Functionalization. *Supramol. Sci.* **1998**, *5*, 41–48.
18. Ghosh, S. K.; Kundu, S.; Mandal, M.; Nath, S.; Pal, T. Studies on the Evolution of Silver Nanoparticles in Micelle by UV-Photoactivation. *J. Nanopart. Res.* **2003**, *5*, 577–587.
19. Joly, S.; Kane, R.; Radzilowski, L.; Wang, T.; Wu, A.; Cohen, R. E.; Thomas, E. L.; Rubner, M. F. Multilayer Nanoreactors for Metallic and Semiconducting Particles. *Langmuir* **2000**, *16*, 1354–1359.
20. Esumi, K.; Suzuki, A.; Yamahira, A.; Torigoe, K. Role of Poly(amidoamine) Dendrimers for Preparing Nanoparticles of Gold, Platinum, and Silver. *Langmuir* **2000**, *16*, 2604–2608.
21. Henglein, A. Reduction of $Ag(CN)_2^-$ on Silver and Platinum Colloidal Nanoparticles. *Langmuir* **2001**, *17*, 2329–2333.
22. Dujardin, E.; Peet, C.; Stubbs, G.; Culver, J. M.; Mann, S. Organization of Metallic Nanoparticles Using Tobacco Mosaic Virus Templates. *Nano Lett.* **2003**, *3*, 413–417.
23. Esumi, K.; Hosoya, T.; Suzuki, A.; Torigoe, K. Formation of Gold and Silver Nanoparticles in Aqueous Solution of Sugar-Persubstituted Poly(amidoamine) Dendrimers. *J. Colloid Interface Sci.* **2000**, *226*, 346–352.
24. Huang, H. Z.; Yang, X. R. Synthesis of Polysaccharide-Stabilized Gold and Silver Nanoparticles: a Green Method. *Carbohydr. Res.* **2004**, *339*, 2627–2631.
25. Yonezawa, Y.; Takami, A.; Sato, T.; Yamamoto, K.; Sasanuma, T.; Ishida, H.; Ishitani, A. Photochemical Formation of Silver Metal-Films from Silver Salt of Natural High Molecular Carboxylic-Acid. *J. Appl. Phys.* **1990**, *68*, 1297–1302.
26. Maillard, M.; Huang, P. R.; Brus, L. Silver Nanodisk Growth by Surface Plasmon Enhanced Photoreduction of Adsorbed $[Ag^+]$. *Nano Lett.* **2003**, *3*, 1611–1615.
27. Rybak, B. M.; Ornatska, M.; Bergman, K. N.; Genson, K. L.; Tsukruk, V. V. Formation of Silver Nanoparticles at the Air-Water Interface Mediated by a Monolayer of Functionalized Hyperbranched Molecules. *Langmuir* **2006**, *22*, 1027–1037.
28. Iloukhani, H.; Bahrami, H. Kinetic Studies and Mechanism on the Permanganic Oxidation of L-Glutamine in Strong Acid Medium in the Presence and Absence of Silver (I). *Int. J. Chem. Kinet* **1999**, *31*, 95–102.
29. Paik, D. H.; Lee, I.-R.; Yang, D.-S.; Baskin, J. S.; Zewail, A. H. Electrons in Finite-Sized Water Cavities: Hydration Dynamics Observed in Real Time. *Science* **2004**, *306*, 671–675.
30. Faust, B. C.; Zepp, R. G. Photochemistry of Aqueous Iron(III) Polycarboxylate Complexes—Roles in the Chemistry of Atmospheric and Surface Waters. *Environ. Sci. Technol.* **1993**, *27*, 2517–2522.
31. Shoeib, T.; Siu, K. W. M.; Hopkinson, A. C. Silver Ion Binding Energies of Amino Acids: Use of Theory to Assess the Validity of Experimental Silver Ion Basicities Obtained from the Kinetic Method. *J. Phys. Chem. A* **2002**, *106*, 6121–6128.
32. Henglein, A. Small-Particle Research: Physicochemical Properties of Extremely Small Colloidal Metal and Semiconductor Particles. *Chem. Rev.* **1989**, *89*, 1861–1873.
33. Keizer, J. Theory of Rapid Biomolecular Reactions in Solution and Membranes. *Acc. Chem. Res.* **1985**, *18*, 235–241.
34. Castanho, M. A. R. B.; Fernandes, M. X. Lipid Membrane-Induced Optimization for Ligand-Receptor Docking: Recent Tools and Insight for the "Membrane Catalysis" Model. *Eur. Biophys. J.* **2006**, *35*, 92–103.
35. Mallick, K.; Jewrajka, S.; Pradhan, N.; Pal, T. Micelle-Catalysed Redox Reaction. *Curr. Sci.* **2001**, *80*, 1408–1412.
36. Ghosh, S. K.; Kundu, S.; Mandal, M.; Pal, T. Silver and Gold Nanocluster Catalyzed Reduction of Methylene Blue by Arsine in a Micellar Medium. *Langmuir* **2002**, *18*, 8756–8760.
37. Hardt, S. L. Rates of Diffusion Controlled Reactions in One, Two and Three Dimensions. *Biophys. Chem.* **1070**, *10*, 239–243.
38. Laszlo, P. Catalysis of Organic-Reactions by Inorganic Solids. *Acc. Chem. Res.* **1986**, *19*, 121–127.
39. Lee, S.-Y.; Royston, E.; Culver, J. M.; Harris, M. T. Improved Metal Cluster Deposition on a Genetically Engineered Tobacco Mosaic Virus Template. *Nanotechnology* **2005**, *16*, S435−S441.
40. Barbas, C. F. *Phage Display:A Laboratory Manual*; Cold Spring Harbor Laboratory Press: Cold Spring Harbor, NY, 2001.
41. Graff, A.; Wagner, D.; Ditlbacher, H.; Kreibig, U. Silver Nanowires. *Eur. Phys. J. D* **2005**, *34*, 263–269.
42. Gilbert, P. U. P. A.; Abrecht, M.; Frazer, B. H. The Organic-Mineral Interface in Biominerals. *Rev. Mineral. Geochem.* **2005**, *59*, 157–185.